Journal of Pharmaceutical Sciences 114 (2025) 103895

Contents lists available at ScienceDirect

Journal of Pharmaceutical Sciences

journal homepage: www.elsevier.com/locate/xphs

Pharmaceutics, Drug Delivery and Pharmaceutical Technology

3D printing personalized medications in a hospital: Rapid and non-destructive dose verification of printed medicines enabled by miniaturised spectroscopy

Anna Kirstine Jørgensen [a], Antoine Dowek [b], Lucas Denis [b], Jun Jie Ong [a], Maxime Annereau [b], André Rieutord [b], Maryam Parhizkar [a,*], Alvaro Goyanes [a,c,d,e,*], Abdul W. Basit [a,d]

[a] Department of Pharmaceutics, UCL School of Pharmacy, University College London, 29-39 Brunswick Square, London, WC1N 1AX, UK
[b] Department of Clinical Pharmacy, Gustave Roussy Cancer Campus, 114 rue Edouard Vaillant, Villejuif, 94800, France
[c] Departamento de Farmacología, Farmacia y Tecnología Farmacéutica, I+D Farma (GI-1645), Facultad de Farmacia, Instituto de Materiales (iMATUS) and Health Research Institute of Santiago de Compostela (IDIS), Universidade de Santiago de Compostela, 15782, Spain
[d] FABRX Ltd., Henwood House, Henwood, Ashford, TN24 8DH, UK
[e] FABRX Artificial Intelligence, Enrique Vidal Abascal 7, Santiago de Compostela, CP 15702, Spain

ARTICLE INFO

Keywords:
Chemometrics for drug quantification
Extrusion-based 3D printing
Process analytical technology
Point of care compounding
Personalised pharmaceuticals
Additive manufacturing of drug products

ABSTRACT

Three-dimensional printing (3DP) of pharmaceuticals is as an enabling technology for personalised medicine and is a versatile production technology for compounding automation and decentralised manufacture. However, non-destructive quality control (QC) methods are needed for the small batch medicines production. This study investigated for the first time two miniaturised and handheld near-infrared (NIR) and Raman spectrometers as QC measures for accurately quantifying tamoxifen in medicines manufactured in Gustave Roussy Cancer Campus Hospital Pharmacy during preparation for a clinical trial. A 'hub-and-spoke' model approach was applied with manufacture of calibration samples in a research environment (i.e. hub or control site) for spectral data acquisition in the hospital pharmacy (i.e. spoke, point-of-care or manufacturing site) for calibration and validation (hospital pharmacy produce) samples containing 30 % w/w tamoxifen citrate, utilising the same suppliers of materials for production. Both NIR and Raman devices yielded highly accurate and predictive models from spectra acquisition into the open capsule bodies and through closed capsule shells and were deemed suitable as QC methods for rapidly determining the tamoxifen content in the medicines produced via pharmaceutical 3DP in the hospital for the clinical trial. This study proved that both miniaturised analysers may be used as non-destructive QC methods for the 3DP medicines production in the hospital pharmacy, and that a 'hub-and-spoke' approach for development of non-destructive chemometric models may accelerate the decentralised or modular manufacturing paradigm of 3DP medications. Future application and implementation of either technology as QC measure at decentralised manufacturing facilities may come down to other factors such as connectivity to in-line, integrated systems, costs, and safety.

Introduction

Three-dimensional (3D) printing of pharmaceuticals has garnered attraction over the past decade for its ability to produce bespoke and small-batch medicines and drug delivery devices.[1–3] Making its way into point of care (PoC) settings such as community and hospital pharmacies, pharmaceutical 3D printing (3DP) offers novel and automated processes for compounding of medicines with enhanced levels of dose control and flexibility and is positively perceived by healthcare professionals.[4–6] Moreover, new legislation is enabling decentralised manufacturing of medicines through 3DP in the United Kingdom, marking a new pharmaceuticals manufacture paradigm.[7] Clinical trials have already confirmed the ability of 3DP to produce personalised oral medicines with positive clinical outcomes and more trials are on the horizon.[8–12]

Quality control (QC) is a vital aspect for release of pharmaceuticals from any given manufacturing process to ensure patient safety and efficacy. To fully benefit from production and dispensing of personalised 3DP oral medicines at the PoC or through small-scale decentralised

* Corresponding authors at: Department of Pharmaceutics, UCL School of Pharmacy, University College London, 29-39 Brunswick Square, London, WC1N 1AX, UK.
E-mail addresses: maryam.parhizkar@ucl.ac.uk (M. Parhizkar), a.goyanes@fabrx.co.uk (A. Goyanes).

https://doi.org/10.1016/j.xphs.2025.103895
Received 22 May 2025; Received in revised form 30 June 2025; Accepted 30 June 2025
Available online 1 July 2025

manufacturing facilities, non-destructive QC measures for analysis of each of the individualised printlets (3DP oral tablets) are required.[13–16] Non-destructive quantitative drug analysis,[17–19] solid-state determination,[20,21] weight uniformity,[22,23] drug and excipient distributions,[24] and porosity assessments[25] for printlets have been published. Near-infrared (NIR) and Raman spectroscopy have been explored for quantitative purposes. Both are vibrational spectroscopic methods capable of conveying quantitative and qualitative sample information and may enable non-destructive dose verification when combined with individual printlet masses. NIR spectroscopy relies on the measure of energy absorbance in a sample through overtones and combination bands from incident polychromatic light,[26] whereas Raman spectroscopy is the measure of inelastic scattering from energy transfer between an incident monochromatic laser beam and the sample.[27]

Spectrometers are usually categorised according to size: Laboratory or benchtop scale, portable (ranging from three to 20 kg), or handheld (less than one kg).[28,29] Although spectrometer size typically is directly related to spectral resolution and sensitivity, and dictates the mode of analysis,[30,31] miniaturised spectrometers may facilitate easier employability in clinical settings and at the PoC as well as faster overall 3DP medicines production rate through potential in-line integration as compared to benchtop or portable equipment. Most published studies have quantified active pharmaceutical ingredients (APIs) in the final printlets through portable, benchtop, and large NIR and Raman spectrometers in research laboratory environments. Handheld NIR spectrometers have been successfully employed in research environments to quantify APIs in printlets produced in research laboratory settings,[32–36] however, no previous studies have proven the feasibility of API quantification in clinical settings through NIR and Raman spectrometers for medicines produced via a pharmaceutical 3D printer in the clinical setting.

Recently, we reported the development of a novel compounding 3DP platform in the hospital pharmacy at Gustave Roussy Cancer Campus in Paris, France, to rapidly and accurately produce thousands of personalised multi-active medicines through a pharmaceutical 3D printer for the purpose of a large clinical study in breast cancer patients.[37] The medicines contained tamoxifen, a first-line therapy for non-menopausal women recovering from breast cancer.[38–44] The tamoxifen pharma-ink (mixture of API and excipients) was produced directly in the hospital pharmacy and deposited into pharmaceutical gelatine capsules through the semisolid extrusion (SSE) technology in the 3D printer. Hence, non-destructively certification of the dose would further enable dispensing of personalised tamoxifen medicines at the hospital pharmacy.

The aim of this study was to investigate the feasibility of using handheld NIR and Raman spectrometers for non-destructive tamoxifen quantification in the 3DP compounded medicines developed for the clinical trial in the Clinical Pharmacy department of Gustave Roussy Cancer Hospital. The two miniaturised spectroscopic techniques should yield rapid and accurate methods to prove the feasibility of using these methods for QC of compounded 3DP medicines in clinical settings. The calibration samples were produced in a research environment (simulating a hub or control site as per the new UK legislation) with the validation samples produced in the hospital pharmacy (the spoke, point of care or decentralised manufacturing site) during the preparation for the clinical trial. Spectral data acquisition was carried out in the clinical facility, highlighting the suitability of the "hub-and-spoke" model for decentralised manufacturing of personalised 3DP pharmaceuticals at the PoC. Here, a centralised hub (i.e. the research environment) could facilitate implementation of non-destructive QC at the spokes (i.e., the hospital pharmacy).

Materials & methods

Materials

Tamoxifen citrate (TC) was obtained from Hepartex® (France), polyethylene glycol (PEG) 4000 was purchased from Merck (United Kingdom), green/white (cap/body) size 0 gelatine capsules (titanium dioxide (TiO_2) content of 2.0 % in body and 1.0 % in cap) were purchased from Cooper® (France). Sodium phosphate monobasic monohydrate ($NaH_2PO_4 \bullet H_2O$), N,N-dimethyloctylamine (DMOA), and acetonitrile (ACN) were purchased from Sigma Aldrich (United Kingdom) and orthophosphoric acid from Thermo Scientific (United Kingdom). 20 mL Injekt® syringes with Luer lock were supplied by B. Braun (Germany). 14 G polypropylene tapered tips (internal diameter of 0.063 inches (1.6 mm)) were purchased from Fisnar® (United States of America).

Production of stainless steel capsule holder

A square holder for size 0 gelatine capsules was manufactured in-house, consisting of two stainless steel layers: a top and a bottom. 25 capsule voids were created on each layer in a five-by-five manner, spaced 25 mm apart centre to centre. On the top layer, the holes were exactly the diameters of the size 0 capsule bodies, while on the bottom layer the voids were half of the capsule diameters. The centres of the top and bottom voids were accurately aligned, and the two layers bolted together.

Preparation of calibration samples

The calibration curve was constructed to span across concentrations from 20 % w/w to 40 % w/w TC (Table 1), as the formulation used in the hospital pharmacy contained 30 % w/w TC.

Pharma-ink preparation for calibration samples

All calibration pharma-inks were prepared according to following procedure. Accurate amounts of PEG 4000 and TC were weighed out separately for a total mass of 5 g per pharma-ink. PEG 4000 was transferred to a beaker which was covered with aluminium foil and placed on a hot plate stirrer at 80 °C until complete melting of PEG 4000. Approximately half of the tamoxifen was added, and the mixture was vortexed for ca. 30 s. A magnetic stirrer bar was added, the beaker was placed back at the hot stirrer plate stirring at 1000 RPM, where the rest of the TC was added and stirred until visibly homogenous (approximately two to three minutes). The molten pharma-inks were immediately transferred to 20 mL Injekt® syringes, capped, covered in aluminium foil, and stored at room temperature until capsule filling.

Filling of capsules via SSE

Calibration capsule samples

The syringe containing pharma-ink was fitted with a 14 G tapered

Table 1
Compositions of pharma-ink formulations for method calibration.

Formulation	TC (%w/w)	PEG 4000 (%w/w)
20.0 % Tamoxifen citrate	20.0	80.0
22.5 % Tamoxifen citrate	22.5	77.5
25.0 % Tamoxifen citrate	25.0	75.0
27.5 % Tamoxifen citrate	27.5	72.5
30.0 % Tamoxifen citrate	30.0	70.0
32.5 % Tamoxifen citrate	32.5	67.5
35.0 % Tamoxifen citrate	35.0	65.0
37.5 % Tamoxifen citrate	37.5	62.5
40.0 % Tamoxifen citrate	40.0	60.0

dispense tip and placed in the SSE printhead attachment for the M3DIMAKER2 3D printer (FABRX, United Kingdom) at 78 °C for 30 min prior to extrusion. Direct extrusion into white size 0 capsule bodies was carried out at 78 °C using the custom-made stainless steel capsule holder for each pharma-ink ($n = 10$ capsules). Approximately 100–250 mg was deposited in each of the calibration capsules, and all capsules were capped with dark green caps.

Hospital pharmacy validation samples

The capsules produced in the Clinical Pharmacy Department of Gustave Roussy Hospital during the preparation for the clinical were used for model validation and QC feasibility. The production method has been described in the previous publication on medicines development by Denis et al.[37] Raw materials and capsule shells used in the present study were from the same suppliers as those used the hospital pharmacy.

Characterisation of raw materials and capsule deposits

Sample preparation

Capsule deposits from four to five capsules per concentrations were emptied into a mortar and pestle and gently crushed into smaller particulates without the use of shearing for subsequent solid-state characterisation of tamoxifen citrate, as described below.

Differential scanning calorimetry (DSC)

DSC measurements were performed on capsule deposits from all calibration concentrations to investigate the solid state of TC as well as the raw TC and PEG 4000 powders. All analyses were performed with a Q2000 DSC (TA Instruments, Waters, USA) with sample sizes of 3–5 mg in TA aluminium pans with Tzero lids using the pinhole method. The samples were equilibrated at 25 °C before being heated up to 160 °C at a heating rate of 10 °C/min. Nitrogen was used as purge gas at 50 ml/min flowrate. Data collection was carried out with TA Advantage software for Q series and analysed using TA Instruments Universal Analysis 2000 (TA Instruments, Waters, USA).

X-ray powder diffraction (XRPD)

XRPD analyses were performed on gently crushed deposits from all calibration samples as well as the raw TC and PEG 4000 powders. All analyses were carried out using a Rigaku MiniFlex 600 (Rigaku, USA) equipped with a CuX199 ray source (lambda = 1.5418 Å). 15 mA and 40 kV intensity and voltage were applied, and samples were scanned between $2\theta = 3 - 60°$ at a speed of 5°/min with 0.02° increments.

Fourier-transform infrared (FT-IR) spectroscopy

FT-IR spectroscopy was performed on raw materials and gently crushed deposits from all calibration capsules. A Spectrum 100 FT-IR spectrometer (PerkinElmer, USA) was used, and samples were scanned over 650–4000 cm^{-1} at a resolution of 4 cm^{-1} for 16 scans.

Spectral acquisition for chemometric model development

36 calibration capsules (four capsules per calibration concentration) and six hospital pharmacy samples were employed for spectral acquisition and chemometric model development and evaluation. To analyse into each of the open capsule bodies, the caps were manually and gently removed and recapped to preserve the physical integrity of the capsule shells. The capsules were opened just prior to and closed immediately following spectra acquisition.

Near infra-red spectroscopy (NIRS)

NIR diffuse reflectance spectra were measured using a MicroNIR 1700ES NIR spectrometer (VIAVI, UK) equipped with 2 vacuum tungsten lamps and an InGaAs photodiode array detector for wavelengths between 950 and 1650 nm (10,526 - 6060 cm^{-1}). All spectra were collected using a tablet probe with 8 mm diameter collection optic (VIAVI, UK) attached to the MicroNIR device and with the MicroNIR Pro software (VIAVI, UK). Prior to data acquisition, a 99 % spectralon reference standard was used for the acquisition of dark and reference spectra for instrument calibration.

Open capsules. Filled capsules without caps were placed in the stainless-steel capsule holder placed on top of the printing platform. The NIR was placed in the NIR attachment for the 3D printer directly over the open capsule at approximately 0.5 mm distance from the top of the capsule to the tip of the probe. All capsules were scanned 10 times with repositioning of the capsule holder between each scan to move capsule within the boundaries of the probe.

Closed capsules. Filled capsules, closed, were placed body (white body) facing upwards on the 99 % spectralon reference standard. The tablet probe was placed over the capsule, and all capsules were scanned three times.

Raman spectroscopy (RS)

Raman reflectance spectra were obtained using a Metrohm Instant Raman Analyzer (MIRA) M-1 (Metrohm, France) equipped with a 785 nm laser covering the spectral range of 400–2300 cm^{-1}. A reference sample was scanned for reference matching value before connection to the software PEAK (Snowy Range Instruments, version 1.1.112) used for data acquisition.

Four different lens adaptors were investigated: three point-and-shoot adaptors with different focal lengths, and a closed vial holder lens. The point-and-shoot lens attachments were the Metrohm short distance lens attachment (SWD) with 1.00 mm focal length, long distance lens attachment (LWD) with 7.6 mm focal length, and the extra-long distance lens attachment (XLWD) with a focal length of 18 mm.

Open capsules. Spectra were obtained by attaching the respective point-and-shoot lens adaptor to the MIRA M-1. The filled capsules without caps were placed in the stainless-steel capsule holder. The MIRA M-1, operated handheld, was held lens facing down into the open white capsule body at an approximate distance of one mm. Each capsule was scanned one time.

Closed capsules. Spectra were obtained by attaching the closed vial lens attachment to the MIRA M-1 and placing the closed capsules inside of the vial holder with the white base of the capsule facing the laser and detector. Each capsule was scanned 3 times.

Pre-processing of spectra and chemometric model development

All spectral processing and chemometric model development was carried out using python (version 3.9.9), a function which is now available in the M3DIMAKER studio software (FABRX, United Kingdom). Specific libraries used included numpy, pandas, matplotlib.pyplot, scipy, sklearn, and math. Investigated preprocessing methods for NIR spectra included standard normal variate (SNV), detrend, multiplicative scatter correction, and derivation through Savitzky-Golay (SG) smoothing method. RS spectra preprocessing included baseline estimation through asymmetric least squares smoothing method and derivation through SG smoothing. The number of latent variables (LVs) to include in the chemometric models were selected through reduction in root mean squared error (RMSE) of fit for calibration and validation samples as a function of LVs as well as the explained spectral variance per LV.

Reference drug loading of capsules

The content of each capsule was accurately weighed, dissolved in mobile phase (see "High-performance liquid chromatography-UV (HPLC-UV)" for composition) in a volumetric flask and diluted with

mobile phase for a nominal tamoxifen base concentration of ca. 0.25 mg/ml. The samples were filtered through 0.22 μm syringe filters (Millipore Ltd, Ireland), and analysed via high-performance liquid chromatography (HPLC) coupled to UV detection, as described in "High-performance liquid chromatography-UV (HPLC-UV)".

High-performance liquid chromatography-UV (HPLC-UV)

Hewlett Packard 1260 Series HPLC system equipped with an online degasser, quaternary pump, column heater, autosampler and UV/Vis detector, was used. 20 μl of the samples were injected into a Hypersil ODS C_{18} 5 μm column, 4.6 × 250 mm (Thermo Scientific, United Kingdom). The mobile phase was prepared by dissolving 506 mg sodium phosphate monobasic monohydrate in 600 ml Type I water, followed by the addition of 3.76 ml N,N-dimethyloctylamine. The pH was adjusted to 3 with orthophosphoric acid, and 490 ml of acetonitrile was added. A flow rate of 1 ml/min was applied, with the column temperature set to 30 °C. Eluents were screened at 240 nm. The calibration curve ranged from 33 μg/ml to 660 μg/ml tamoxifen base ($R^2 = 0.9999$, LoD = 5.3 μg/ml, LoQ = 16 μg/ml).

Statistical analysis

Paired *t* tests were conducted between the TC concentrations established by HPLC and as predicted by the developed NIR and Raman models, respectively, for the capsules produced in the Clinical Pharmacy Department of Gustave Roussy Cancer Hospital ($n = 6$) to assess if the means were significantly different ($p < 0.05$).

Results & discussion

Drug loading of capsules for chemometric model development

All capsules included in the chemometric model development were subjected to drug loading determination via HPLC once all the spectra had been obtained via NIR and Raman. These HPLC determined drug loading values (Table 2) were used to develop the chemometric models.

The results of the drug loading for all calibration and external validation capsule deposits are presented in Table 2. Generally, a low relative standard deviation (RSD) was observed for the content of all capsule deposits. Only two capsule formulations had RSD's just above 2 %, whilst all other formulations have RSD's of <1.2 %, indicating that homogenous formulations were obtained during pharma-ink preparation. The pharma-ink for the capsules produced in the hospital pharmacy were produced in larger batches, potentially accounting for the slightly higher deviation for this formulation. Moreover, none of the calibration capsules varied >2 % from the theoretical drug loading, ensuring an even distribution of calibration points for the chemometric models whilst small deviations within each concentration group were captured.

Table 2
HPLC determined drug loading of all calibration and Hospital Pharmacy (*) tamoxifen citrate capsule deposits along with relative standard deviation.

Nominal TC conc. (% w/w)	Number of capsules	Actual TC conc. (% w/w)	RSD (%)
20.0	4	20.08 ± 0.16	0.79
22.5	4	22.51 ± 0.57	2.54
25.0	4	24.84 ± 0.28	1.11
27.5	4	27.21 ± 0.28	1.04
30.0	4	29.65 ± 0.27	0.90
32.5	4	31.96 ± 0.36	1.14
35.0	4	34.52 ± 0.40	1.16
37.5	4	37.08 ± 0.25	0.68
40.0	4	40.04 ± 0.11	0.27
30 *	6	30.73 ± 0.70	2.28

Characterisation of raw materials and capsule contents

Solid-state analyses were performed on gently crushed deposits from all calibration samples to confirm that the pharma-ink preparation and 3DP capsule filling did not alter the polymorphic form of TC to ensure accurate chemometric model development.

The thermograms for all calibration samples as well as raw tamoxifen citrate and PEG 4000 powders are presented in Fig. 1. Pure TC showed a melting endotherm at 147.5 °C, whilst the melting endotherm for PEG 4000 showed at 59.6 °C. Melting point suppression for TC was observed for all calibration samples, confirming that TC was still present to some degree in a crystalline form, whilst partially being molecularly dispersed in the polymer. TC melting points ranged from 136.6 °C to 141.3 °C across the concentration range, and the observed melting point depression was greater at higher ratios of PEG 4000 to TC, indicating some degree of TC solubilisation under the application of heat during the thermogram acquisitions. DSC analysis indicated that pure TC particles contained the polymorphic Form A, however, due to solubilisation in the polymer, the polymorphic determination of TC in calibration samples could not be confirmed through DSC analysis.

The XRPD diffractograms of raw materials TC and PEG 4000 along with all calibration samples are presented in Fig. 2. XRPD analysis confirmed that pure TC constituted the polymorphic Form A, as compared to unique diffraction patterns previously reported on the polymorphic form.[45] Particularly the absence of a large diffraction peak at ca. 5.5° 2θ and the distinctive peak shapes and intensities observed at ca. 11.5° and 13.8° 2θ indicate the presence of Form A. XRPD data obtained for all the calibration samples confirmed the presence of TC in a crystalline form, and the data indicated the continued presence of TC Form A, as seen from the characteristic peaks in the range of ca. 9–18° 2θ, in all developed samples. Small differences in relative intensities and slight peak broadenings observed for the samples from capsule deposits may have been a result of sample preparation resulting in particulates larger than those for pure TC and PEG 4000 materials.[46] The DSC and XRPD analyses confirmed that TC was present in the same crystalline form in the calibration samples as in the medicines produced in the hospital pharmacy, as we previously reported the characterisation data for these.[37]

Moreover, analysing the acquired FT-IR spectra of TC powder confirmed the presence of the polymorphic Form A, indicated by a characteristic sharp C=O acid group stretch at 1730 cm^{-1} followed by a broadened asymmetric stretch of the -COO^- ion at 1587 cm^{-1} (Fig. 3).[47] Moreover, the unique absorbances bands at 1241 cm^{-1} (aromatic ring, para-substituted), 1217 cm^{-1} (aromatic ring, para-substituted), and 1173 cm^{-1} (C—O stretch) as well as a sharp absorbance at 703 cm^{-1} (aromatic ring, mono-substituted) further indicated the polymorphic Form A.[47] All mentioned peaks were observed in the FT-IR spectra for calibration (Fig. 3).

The performed analytical characterisation confirmed that manufacturing of the calibration and hospital pharmacy samples at different scales had not resulted in altered physical form of TC or interactions in the capsule deposits. Thus, the calibration samples were suitable for inclusion in the chemometric model development process in the "hub-and-spoke" setup.

Chemometric models for tamoxifen quantitation

Tamoxifen content prediction through closed capsules

All closed capsules were scanned through their white capsule bodies after production of all the calibration and hospital pharmacy capsules. For both NIRS and RS, the best performing models were obtained through the inclusion of the full spectra, covering the wavenumbers 6061 - 10,526 cm^{-1} and 400 - 2300 cm^{-1}, respectively. For the NIRS model, all spectra were subjected to pre-processing constituting of scatter correction via SNV (Fig. 4B) and smoothing and derivative through SG method (width (w) = 5, polynomial (p) = 2, derivative (D) =

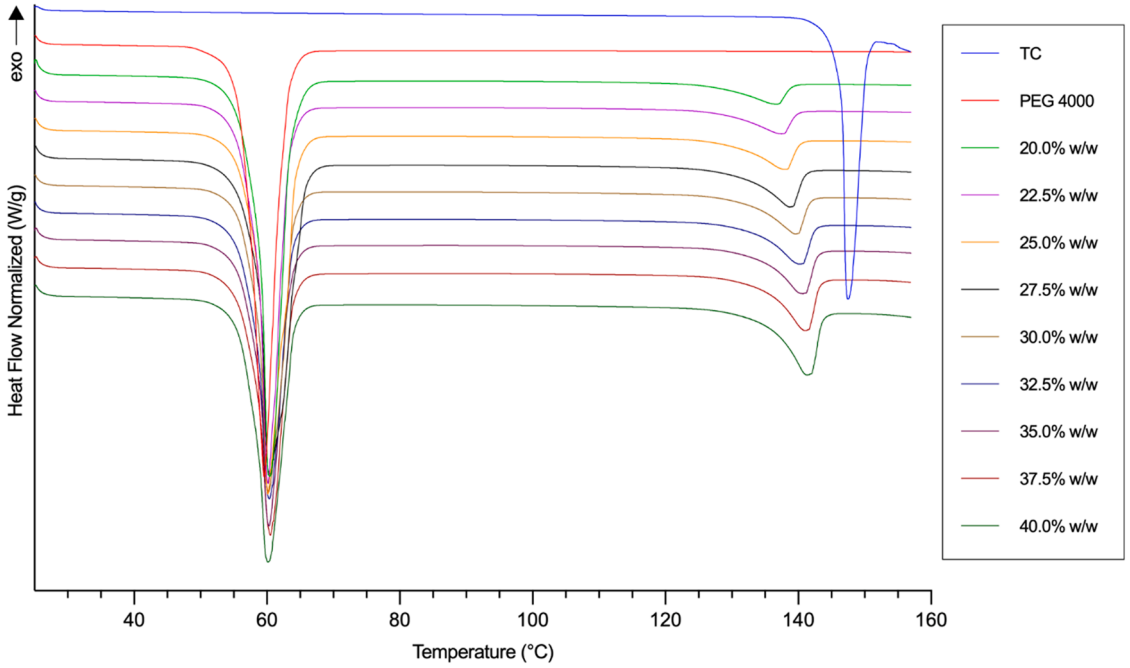

Fig. 1. DSC thermograms of pure TC and PEG 4000 as well as all calibration samples.

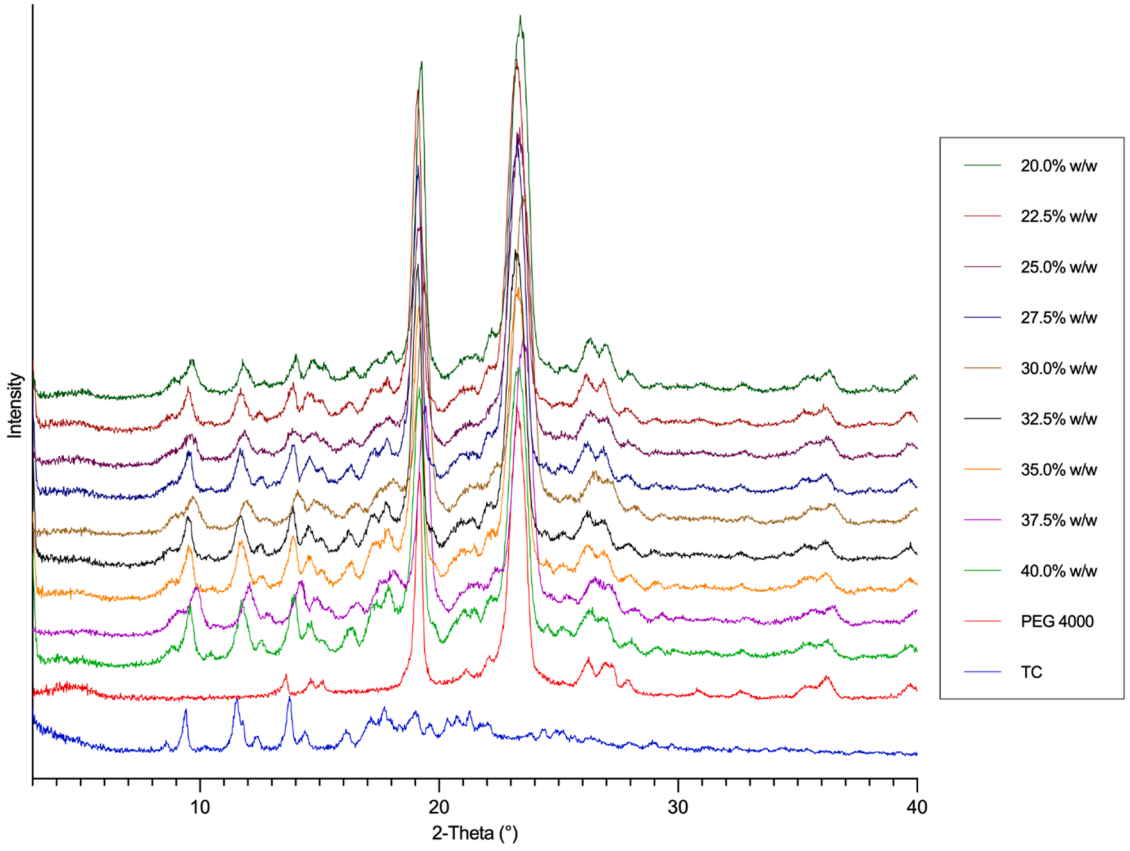

Fig. 2. XRPD diffractogram of pure TC and PEG 4000, and calibration samples.

2) (Fig. 4C). A Partial Least Squares Regression (PLSR) model with 4 LV's was found to result in the best performing model assessed on goodness of fit and prediction accuracy (Fig. 4D). Specifically, the co-efficient of determination (R^2) was 0.956 for the calibration set and 0.793 upon being subjected to a 10-fold cross validation (CV). The root mean square error of calibration (RMSEC) was found to be 1.33 % w/w whilst the model accuracy (root mean square error of prediction (RMSEP)) was 1.19 % w/w for the hospital pharmacy samples. This corresponds to a relative error of 3.9 % for capsules produced in the hospital pharmacy when compared to HPLC determined TC content of

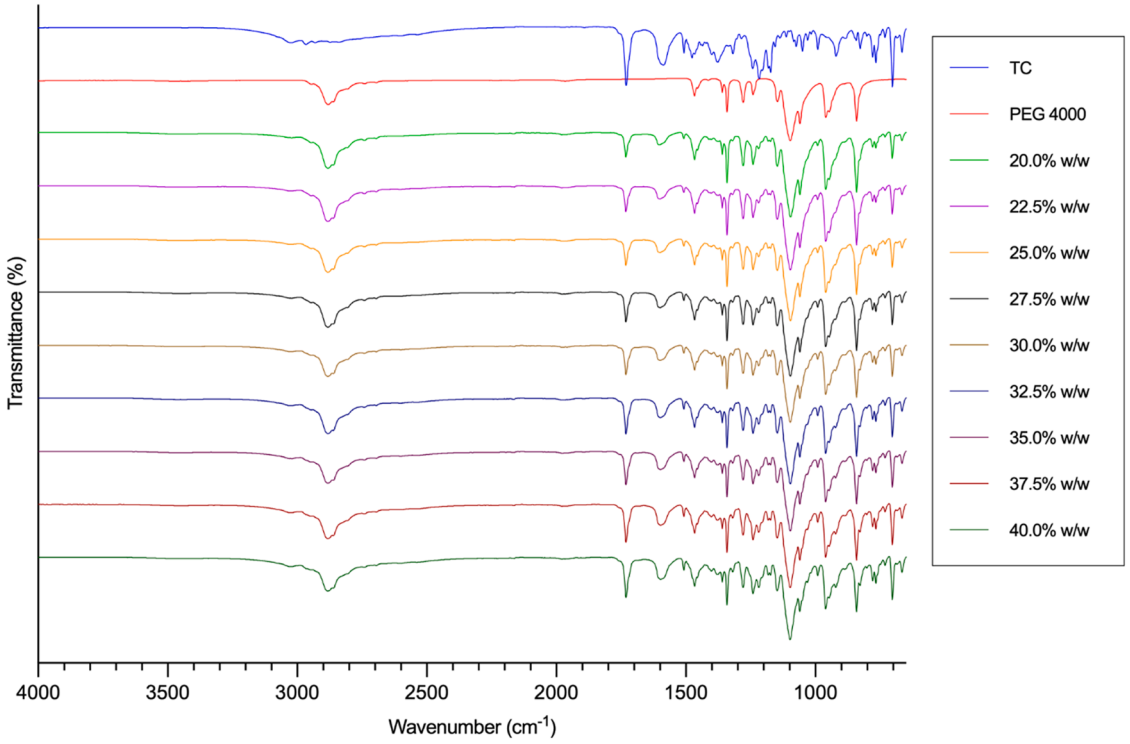

Fig. 3. FT-IR spectra of all samples, including raw material TC and PEG 4000, along with samples from calibration deposits.

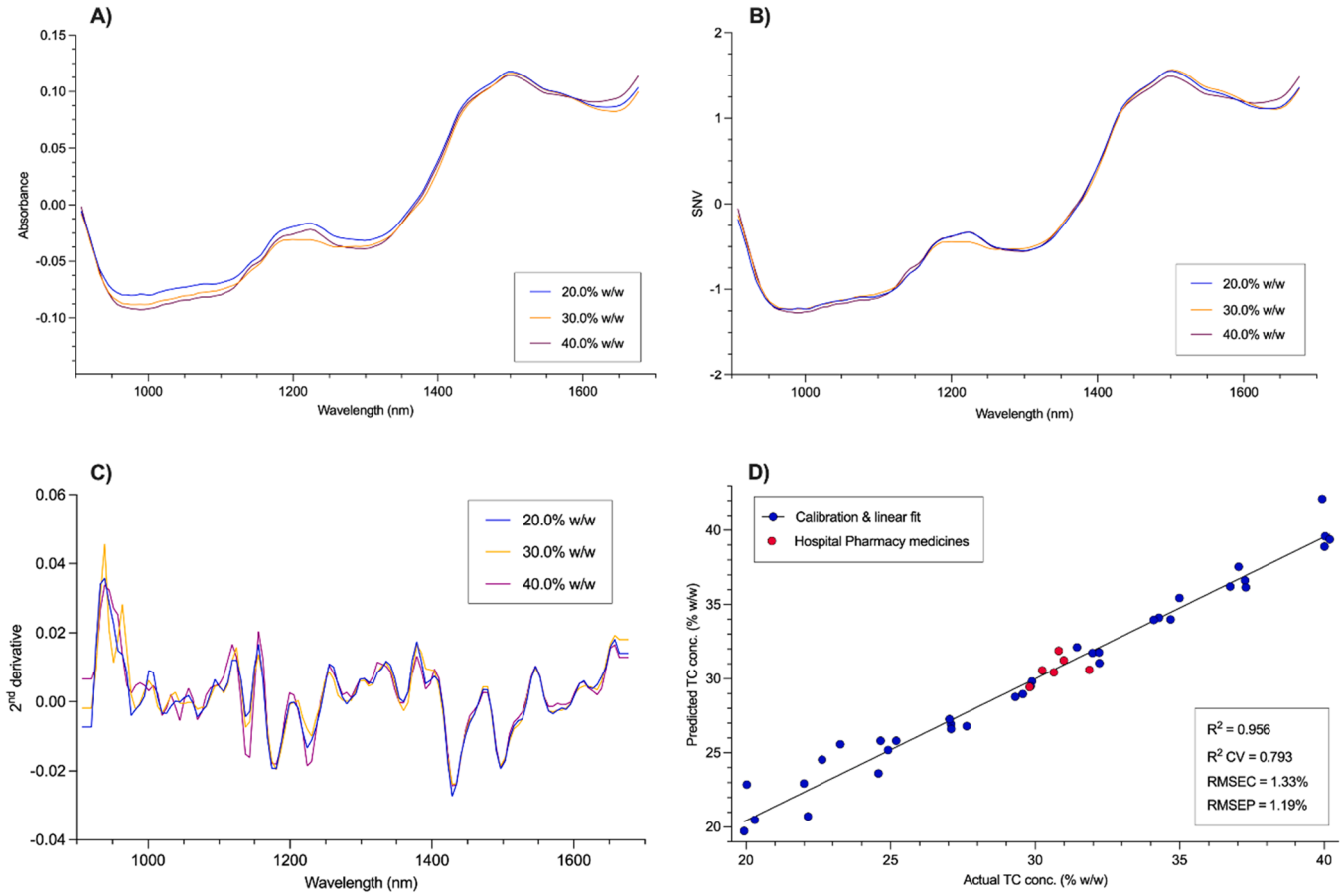

Fig. 4. Selected raw and pre-processed NIR spectra (one spectrum per 20 %, 30 %, and 40 % calibration samples) for acquisition through closed capsules along with developed PLSR model with 4 latent variables. (A) Raw spectra, (B) spectra subjected to SNV scatter correction, (C) 2nd derivative spectra following SNV and SG smoothing, and (D) developed PLSR model with 4 LVs.

the capsules.

A recently published study utilised a portable NIR system for detection and quantification of APIs through capsules and found that spectral variance was influenced by capsule type and capsule colour as well as API type, thus highlighting the importance of consistency in capsule provider for the developed model as was factored in for this study.[48] The developed NIR model in this work performed similarly to NIR models developed for quantifying saponins in traditional Chinese medicine capsules in closed capsules when assessed on relative prediction error on external validation set (here, the hospital pharmacy produced samples) as well as hydrocortisone in capsules when assessed on goodness of fit of the calibration samples.[49,50] Both referenced studies were carried out with benchtop scale instruments, hence a significant reduction in instrument size was achieved here.

For RS, all spectra were subjected to baseline estimation via asymmetric least squares (ALS) algorithm by optimising the smoothness (lambda) and asymmetry (p) factors (lambda $= 10^9$, $p = 0.01$) ,[51] and smoothing and derivative through the SG method ($w = 17, p = 2, D = 1$). A PLSR model with 3 LVs showed best goodness of fit to calibration data ($R^2 = 0.923$, RMSEC = 1.762 % w/w). However, the model experienced a drastic decrease in R^2 upon 10-fold CV (R^2 CV = 0.691). The RMSEP for the hospital pharmacy medicines (1.11 % w/w) was equal to that obtained through NIRS, equivalent to 3.6 % relative error.

A benchtop transmission Raman spectrometer for API quantification through closed capsule bodies of conventionally filled pharmaceutical capsules has previously been investigated.[52] The model was developed with a consistent fill level (100 mg) in white body and red cap gelatine capsules over a range of 67.5 % w/w to 82.5 % w/w API but was employed for the prediction of varying fill levels (100 to 400 mg) in gelatine capsules of different colours. The authors reported a developed model with RMSEP = 1.1 % w/w, corresponding to 1.5 % relative error assessed on target fill levels (100 mg) of the formulation containing 75 % w/w API, whilst higher fill levels increased the relative prediction error to 2 – 9 %, irrespective of capsule colour.[52] Considering the 2.5 times difference in target levels API (75 % w/w against 30 % w/w) and the greater specifications of the benchtop transmission Raman system (5–6 cm^{-1} resolution, 1.5 W laser power, 125 mm focal length, and laser wavelength of 830 nm) compared to those of the handheld MIRA M-1 (resolution of 16–18 cm^{-1}, <100 mW laser power, and 785 nm laser wavelength), the prediction accuracies were not vastly different.[53–55] The reflectance operation of the handheld MIRA device may also have played a role in the decreased performance of the developed model in this study as compared to the model developed with transmission Raman spectra, due to increased signal detection, and potentially induced fluorescence, arising from the capsule shells.[54,56–58] Lastly, a greater number of capsules per API concentration were included in the referenced study (10 capsules per calibration concentration) against those included in this study (four capsules per calibration concentration), leading to a more robust and generalisable model.

A different study reported on backscatter Raman analysis of APIs in closed capsules and found that capsule shells of different colours such as yellow, red, and blue were more prone to fluorescence induction and signal deterioration as compared to white or colourless capsule shells.[58] This finding is further in favour of using white capsule bodies for non-destructive quantification of the medicines manufactured via a pharmaceutical 3DP at the PoC for the clinical trial or as part of a decentralised manufacturing process. The presence of TiO_2 in the capsule shells may also have been responsible for reduced goodness of fit upon CV for both NIR and RS models due to enhanced light scattering, an often desirable feature for prevention of API degradation and visual content masking.[48,59,60]

Tamoxifen content prediction through open capsules

Detrend pre-processing with a breakpoint at the first spectral point for NIR spectra acquired by scanning into the open capsules along with 2nd derivation through SG smoothing ($w = 15$, $p = 2$) was applied for the resulting PLSR model. All spectral points were included in the development of the PLSR model (4 LVs). Intensified absorbance values at higher wavelengths are often observed for NIR spectra of solids due to combination absorbance bands, and the use of detrending, a frequently employed scatter correction technique for NIRS, can be useful to remove the baseline effects of these by fitting and subtracting a, usually second order, polynomial to the signal.[61–63]

A slight increase in coefficient of determination ($R^2 = 0.965$) was obtained compared to scanning through closed capsules, along with an increase in R^2 upon 10-fold CV was obtained (R^2 CV = 0.880), indicating a more robust model. The RMSEC was 1.53 % w/w and the prediction accuracy 1.74 % w/w for the hospital pharmacy samples, corresponding to a relative error of 5.7 %. Overall, this indicates a more robust model with better predictive capacities. The slight increase in RMSEC and RMSEP compared to scanning through closed capsules may be a consequence of spectra acquisition into the open capsules at a very slight distance from the capsule shell, potentially leading to signal loss to the environment as well as signal arising from the environment (i.e. the capsule holder), although it could also be due to the increased number of datapoints included in the model. A summary of the applied chemometrics and developed NIR models for both sample presentation modes is presented in Table 3.

Three different point-and-shoot lens adaptors were explored for Raman spectra acquisition into open capsules: the SWD lens with a 1.00 mm focal length, the LWD lens with a 7.6 mm focal length, and the XLWD lens with an 18 mm focal length. Raw and pre-processed spectra obtained from the application of the XLWD lens adaptor are presented in Fig. 5. Pre-processing consisted of ALS baseline estimation (lambda $= 10^7$, $p = 0.05$) and SG derivation ($w = 9, p = 2, D = 1$). The PLSR (4 LVs) model was developed with the spectral points from 750–1750 cm^{-1}.

A scatter plot depicting the correlation between actual TC concentration in calibration and validation capsules against the PLSR (4 LVs) predicted concentrations through Raman spectra obtained with the MIRA M-1 and XLWD lens attachment are presented in Fig. 5D The calibration model showed excellent linearity both on full calibration set ($R^2 = 0.998$) and upon 10-fold CV by leave-one-out ($R^2 = 0.951$), indicative of a very robust model. Furthermore, a low RMSEC was observed at 0.265 % w/w, whilst the RMSEP was only 1.00 % w/w for the hospital pharmacy medicines, corresponding to a relative error of 3.3 % w. Thus, a very robust and accurate model was obtained through Raman spectra acquisition with the MIRA M-1 equipped with the XLWD lens adaptor. Generally, all three lens adaptors for the MIRA M-1 yielded highly linear models with good predictive performances (Table 3), which may be due to the Orbital Raster Scan (ORS) technology implemented in the instrument. ORS enables the analysis of a larger sample surface whilst preserving good instrument spatial resolution and sensitivity.[64]

Increasing the focal length of the Raman spectrometer by changing the lens adaptors should lead to higher spatial resolution and thus better chemometric models.[53,65] However, the focal length of the adaptors did not seem to impact the generated models as the XLWD and SWD lenses resulted in models with nearly equal goodness of fit and predictive capabilities (Table 3). The handheld instrument operation may have been responsible for the LWD model performing worse than the two other lens adaptors. The capsule fill level has been reported as insignificant for API quantification through closed capsule bodies with a benchtop transmission Raman.[52] However, for reflectance Raman spectra acquisition into the open capsules from above, fill level and shape may play an important role for sample-to-detector distance, and thereby influence the resulting chemometric models if these are not appropriately eliminated through pre-processing.[66] Mostly, the handheld aspect of this acquisition mode may have induced further differences in sample-to-detector distance, influencing the resulting quantitative models.[67]

Table 3
Summary of pre-processing parameters and selected LV for PLSR model development and evaluation metrics for each acquisition mode (open and closed capsules) for handheld NIRS and RS instruments.

Parameter	Mode (lens)	Scatter correction & baseline estimation	SG	Spectral points*	LV	Goodness of fit	Accuracy (RMSEP)
NIR	Closed	SNV	$w = 5, p = 2, D = 2$	All	4	$R^2 = 0.956$, R^2 CV = 0.793, RMSEC = 1.33 %	1.19 %
	Open	Detrend, ($bp = 1$)	$w = 15, p = 2, D = 2$	All	4	$R^2 = 0.965$, R^2 CV = 0.880, RMSEC = 1.53 %	1.74 %
Raman	Closed (vial)	Baseline, ($l = 10^9, p = 0.01$)	$w = 17, p = 2, D = 1$	All	3	$R^2 = 0.923$, R^2 CV = 0.691, RMSEC = 1.762 %	1.11 %
	Open (SWD)	Baseline, ($l = 10^7, p = 0.05$)	$w = 9, p = 2, D = 1$	750–1750 cm^{-1}	3	$R^2 = 0.992$, R^2 CV = 0.947, RMSEC = 0.581 %	0.97 %
	Open (LWD)	Baseline, ($l = 10^4, p = 0.01$)	$w = 9, p = 2, D = 1$	750- 1750 cm^{-1}	4	$R^2 = 0.987$, R^2 CV = 0.881, RMSEC = 0.728 %	1.80 %
	Open (XLWD)	Baseline, ($l = 10^7, p = 0.05$)	$w = 9, p = 2, D = 1$	750- 1750 cm^{-1}	4	$R^2 = 0.998$, R^2 CV = 0.951, RMSEC = 0.265 %	1.00 %

Abbreviations: SNV – standard normal variate; bp – breakpoint; l – lambda; p (scatter correction column) – asymmetry factor; SG – Savitzky-Golay; w = filter width; p (SG column) – polynomial; D – derivative; LV – latent variables; CV – cross validation.
* Spectral points refer to the selected spectral points (wavenumbers).

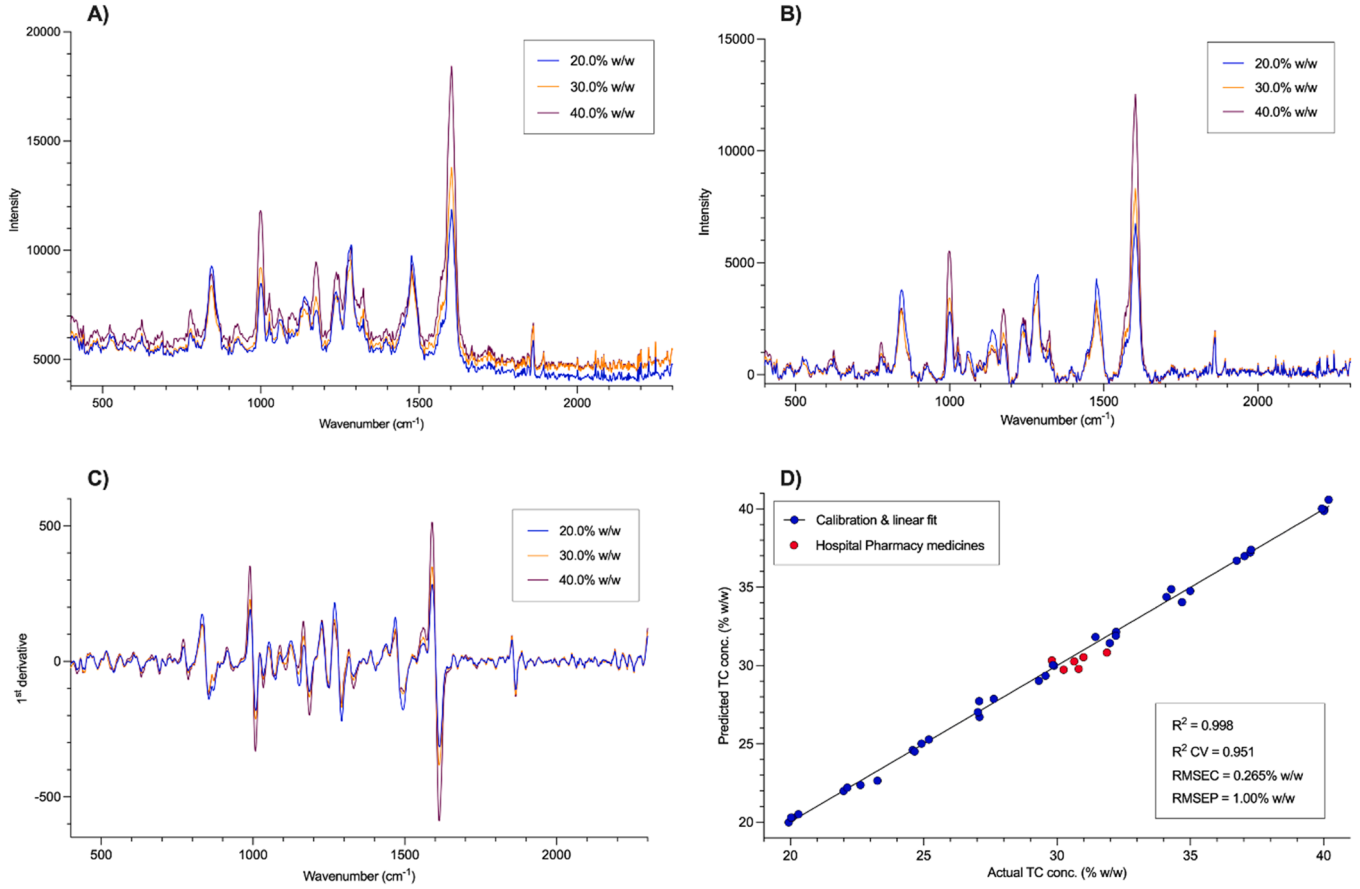

Fig. 5. Selected raw and pre-processed Raman spectra (one spectrum per 20 %, 30 %, and 40 % calibration samples) from acquisition into open capsules with XLWD lens adaptor along with developed PLSR model. (A) Raw spectra, (B) spectra subjected to baseline estimation via ALS, (C) 1st derivative spectra following baseline estimation, and (D) developed PLSR model with 4 LVs.

Tamoxifen quantification in hospital pharmacy compounded medicines

It is vital to determine the dose of API in medicines to be given to patients. Fruitful discussions between pharmaceutical 3DP stakeholders and regulatory authorities (such as the U.S. Food and Drug Administration (FDA),[68] U.K. Medicines and Healthcare products and Regulatory Agency (MHRA),[69,70] and European Medicines Agency (EMA)[71]) have yielded publications on the potentiality of 3DP as part of a decentralised pharmaceutical manufacturing paradigm. Until now, reference to available pharmacopeial monographs for conventional pharmaceuticals have mostly been applied in existing cases of clinical studies on medicines produced by 3DP as specific guidelines had not yet been formalised.[8,10,11] Early 2025, the UK government signed into law the amendment "Modular Manufacture and Point of Care" to The Human Medicines Regulations Statutory Instruments 2025 no 87 in

which 3DP of personalised medicines will fall under the Modular Manufacturing umbrella with respective Control Sites (i.e. hubs) and Modular Manufacturing Sites (i.e. spokes).[72] Coming into effect on 23rd July 2025, this shift in paradigm of medicines manufacturing is set to transform the landscape of personalised therapy through 3DP.

For personalised printlets and small-batch purposes of medicines produced from 3DP, it is important to verify the dose of each individual dosage unit as statistical inference methods remain infeasible. The predicted TC concentration in each capsule produced in the Clinical Pharmacy Department of Gustave Roussy hospital from the NIRS and RS PLSR models are presented in Fig. 6. No statistical difference was found for predicting TC concentration through closed capsules by NIRS (p = 0.9048) nor RS (p = 0.1192) models compared to the reference HPLC method. Similarly, models developed from spectra acquisition into open capsules showed no statistically significant differences for NIRS (p = 0.1790), RS with SWD (p = 0.2838) and XLWD lenses (p = 0.2819), although significant differences were found for RS with LWD lens attachment (p = 0.0002). Hence, both miniaturised spectroscopic methods would be suitable as non-destructive QC methods for TC quantification in the hospital for the capsules filled via pharmaceutical 3DP

Dose verification through NIRS and RS will only be applicable if the mass of each dosage unit can also be determined alongside the concentration determination from the chemometric models. Here, acceptance limits for tamoxifen dose were applied based on U.S. pharmacopoeia requirements, stating that for conventional TC tablets, tamoxifen doses should remain within 90 to 110 % of the labelled amount. The mass of TC deposit in each of the capsules produced at the hospital pharmacy was determined off-line with an analytical balance, and hence the tamoxifen dose was verified in all instances. Recently, the in-line integration of analytical balances within pharmaceutical 3D printers have been reported, meaning that the mass of the printlets produced could be assessed in real-time for instant dose uniformity assessments, yielding an automated production and partial QC process.[5,23,73] In the future, miniaturised spectroscopic analysers, such as those investigated in this work, may also be integrated in-line within pharmaceutical 3D printer systems alongside an analytical balance, which would allow for in-line QC such as dose, immediately verifying the appropriateness for dispensing of the printlets to patients. Such automated systems hold the potential to significantly improve the prospect of personalised medicines from both patient, healthcare professionals, manufacturer, and socioeconomic perspectives.[74]

As both techniques and spectra acquisition methods proved suitable in TC quantification in the capsules, the decision whether to utilise miniaturised NIR or Raman analysers going forward may be influenced by other aspects. First, if the overall aim is in-line integration of the spectroscopic analyser within the printer system for an automated production and QC process, it may depend on whether the analyser can be controlled using third-party software (i.e. software also controlling 3D printer). For this purpose, scanning into open capsule bodies would be the likely scenario through spectra acquisition in similar fashion to the capsule filling process (i.e. through a movable attachment), whereas scanning through closed capsule bodies would likely require manual handling and operation. In addition, user safety may also guide future selection. Raman analysers contain and rely on monochromatic laser radiation and depending on the class of laser in the system, additional personal protective equipment may need to be considered for operating staff and anyone in vicinity of the laser.[75] Lastly, depending on the use-cases of the 3D printer (i.e. at hospital or community pharmacies vs as part of a decentralised manufacturing scheme), costs of the spectroscopic analysers may potentially also be a factor guiding selection.

Developing chemometric models may often lie outside the capacity of healthcare professionals, hence this is an aspect that requires consideration for implementation feasibility. Chemometric model development services could be performed by third-parties or as part of the "hub-and spoke" framework (i.e. through chemometrics professionals at the 'hub' overseeing and guiding multiple 'spokes'). Another likely scenario is automated chemometric model development powered by integrated 'intelligent' healthcare software controlling the entire 3D printing systems, with appropriate controls in place according to existing regulation.

The results obtained in this study confirm the applicability and feasibility of the "hub-and-spoke" model for QC of decentralised or distributed manufacturing of personalised medicines produced by pharmaceutical 3DP. The presented results highlight that the production of calibration samples for chemometric model development may be carried out a hub (control site, here, research environment) whilst spectra acquisition for model development and deployment may be accomplished at a spoke (manufacturing site, here, the Gustave Roussy Hospital Pharmacy) for successful dose determination at the PoC manufacturing facility (or modular manufacturing facility according to the new UK legislation[72]).

Conclusion

For the first time, two miniaturised, handheld NIR and Raman spectroscopic analysers were assessed as a non-destructive QC method for rapid tamoxifen quantification in personalised medicines

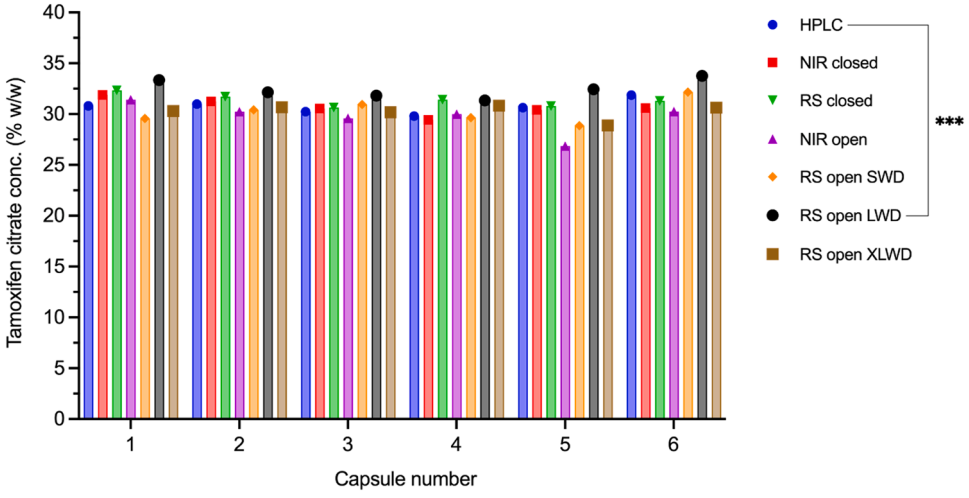

Fig. 6. TC concentration in each individual capsule produced in the Clinical Pharmacy department predicted by the developed NIR and Raman XWLD models for spectra acquisition into open capsules compared to reference quantitation by HPLC. * Indicative of statistically significant differences.

manufactured via a 3D printer in a hospital pharmacy for a clinical trial. Spectra acquisition both from above into the open capsules and through the closed capsule shells yielded highly linear and predictive PLSR models for both NIR and Raman spectrometers. Both NIR and Raman models were capable of accurately determining the tamoxifen concentration in each dosage unit produced in the hospital pharmacy with no statistically significant differences for predicted concentrations when compared to the established HPLC method for all models but one point-and-shoot Raman model. Both NIR and Raman models were suitable to determine if the dose units produced at Gustave Roussy hospital pharmacy contained appropriate tamoxifen doses for the participants of the clinical trial when combined with weights of the tamoxifen deposits recorded manually, off-line for each capsule. This work demonstrates the feasibility of accurately quantifying API in compounded capsules in a clinical setting by miniaturised spectrometers for non-destructive and rapid analysis. In addition, the feasibility of developing non-destructive quantitation models for use at the PoC through a 'hub-and-spoke' framework was proven through calibration sample manufacture at the 'hub' (i.e. control site) with spectra acquisition and model employment for QC at the 'spoke' (i.e. manufacturing site).

Funding

A.K.J. acknowledges the Engineering and Physical Sciences Research Council (EPSRC) UK for their financial support (EP/S023054/1). This research was partially funded by Xunta de Galicia [ED431C 2024/09] and by Ministerio de Ciencia, Innovacion y Universidades (PID2023–149544OB-C22).

Declaration of competing interest

The authors declare the following financial interests/personal relationships which may be considered as potential competing interests: The authors declare the following financial interests/personal relationships which may be considered as potential competing interests: Abdul W. Basit reports a relationship with FABRX Ltd. that includes: employment and equity or stocks. Alvaro Goyanes reports relationships with FABRX Ltd. and FABRX Artifical Intelligence that include: employment and equity or stocks.

Acknowledgments

Graphical abstract created with BioRender.com.

Data availability

Data will be made available upon reasonable request.

References

1. Tracy T, Wu L, Liu X, Cheng S, Li X. 3D printing: innovative solutions for patients and pharmaceutical industry. *Int J Pharm*. 2023;631:122480.
2. Ragelle H, Rahimian S, Guzzi EA, Westenskow PD, Tibbitt MW, Schwach G, et al. Additive manufacturing in drug delivery: innovative drug product design and opportunities for industrial application. *Adv Drug Deliv Rev*. 2021;178:113990.
3. Englezos K, Wang L, Tan E, Kang L. 3D printing for personalised medicines: implications for policy and practice. *Int J Pharm*. 2023;635:122785.
4. Sandler Topelius N, Shokraneh F, Bahman M, Lahtinen J, Hassinen N, Airaksinen S, et al. Automated non-sterile pharmacy compounding: a multi-site study in European hospital and community pharmacies with pediatric immediate release propranolol hydrochloride tablets. *Pharmaceutics*. 2024;16(5):678.
5. Rodríguez-Maciñeiras X, Bendicho-Lavilla C, Rial C, Garba-Mohammed K, Worsley A, Díaz-Torres E, et al. Advancing medication compounding: use of a pharmaceutical 3D printer to auto-fill minoxidil capsules for dispensing to patients in a community pharmacy. *Int J Pharm*. 2025;671:125251.
6. Levine VR, Paulsson M, Stromme M, Quodbach J, Lindh J. Off-the-shelf medication transformed: custom-dosed metoprolol tartrate tablets via semisolid extrusion additive manufacturing and the perception of this technique in a hospital context. *Int J Pharm X*. 2024;8:100277.
7. Jørgensen AK, Goyanes A, Basit AW. Entering new domains for 3D printing of drug products. *Pharm Technol*. 2025;49(3):24–27.
8. Rodríguez-Pombo L, de Castro-López MJ, Sánchez-Pintos P, Giraldez-Montero JM, Januskaite P, Duran-Piñeiro G, et al. Paediatric clinical study of 3D printed personalised medicines for rare metabolic disorders. *Int J Pharm*. 2024;657:124140.
9. Goyanes A, Madla CM, Umerji A, Duran-Piñeiro G, Giraldez-Montero JM, Lamas-Días MJ, et al. Automated therapy preparation of isoleucine formulations using 3D printing for the treatment of MSUD: first single-centre, prospective, crossover study in patients. *Int J Pharm*. 2019;567:118497.
10. Lyousoufi M, Lafeber I, Kweekel D, de Winter BCM, Swen JJ, Le Brun PPH, et al. Development and bioequivalence of 3D-printed medication at the point-of-care: bridging the gap toward personalized medicine. *Clin Pharmacol Ther*. 2023;113(5):1125–1131.
11. Liu L, Fu K, Hong S, Wang Z, Mo M, Li S, et al. Improving the quality and clinical efficacy of subdivided levothyroxine sodium tablets by 3D printing technology. *J Drug Deliv Sci Technol*. 2023;89:105008.
12. Rodríguez-Pombo L, Gallego-Fernández C, Jørgensen AK, Parramon-Teixidó CJ, Cañete-Ramirez C, Cabañas-Poy MJ, et al. 3D printed personalized therapies for pediatric patients affected by adrenal insufficiency. *Expert Opin Drug Deliv*. 2024;21(11):1–17.
13. Jørgensen AK, Ong JJ, Parhizkar M, Goyanes A, Basit AW. Advancing non-destructive analysis of 3D printed medicines. *Trends Pharmacol Sci*. 2023;44(6):379–393.
14. Deon M, dos Santos J, de Andrade DF, Beck RCR. A critical review of traditional and advanced characterisation tools to drive formulators towards the rational development of 3D printed oral dosage forms. *Int J Pharm*. 2022;628:122293.
15. Edinger M, Jacobsen J, Bar-Shalom D, Rantanen J, Genina N. Analytical aspects of printed oral dosage forms. *Int J Pharm*. 2018;553(1):97–108.
16. Forbes TP, Gillen JG, Feeney W, Ho J. Quality by design considerations for drop-on-demand point-of-care pharmaceutical manufacturing of precision medicine. *Mol Pharm*. 2024;21(7):3268-3280.
17. Trenfield SJ, Goyanes A, Telford R, Wilsdon D, Rowland M. Gaisford S., et al. 3D printed drug products: non-destructive dose verification using a rapid point-and-shoot approach. *Int J Pharm*. 2018;549(1):283–292.
18. Trenfield SJ, Tan HX, Goyanes A, Wilsdon D, Rowland M. Gaisford S., et al. Non-destructive dose verification of two drugs within 3D printed polyprintlets. *Int J Pharm*. 2020;577:119066.
19. Edinger M, Iftimi LD, Markl D, Al-Sharabi M, Bar-Shalom D. Rantanen J., et al. Quantification of inkjet-printed pharmaceuticals on porous substrates using Raman spectroscopy and near-infrared spectroscopy. *AAPS PharmSciTech*. 2019;20(5):207.
20. Trenfield SJ, Januskaite P, Goyanes A, Wilsdon D, Rowland M. Gaisford S., et al. Prediction of solid-state form of SLS 3D printed medicines using NIR and Raman spectroscopy. *Pharmaceutics*. 2022;14(3):589.
21. Fanous M, Bitar M, Gold S, Sobczuk A, Hirsch S. Ogorka J., et al. Development of immediate release 3D-printed dosage forms for a poorly water-soluble drug by fused deposition modeling: study of morphology, solid state and dissolution. *Int J Pharm*. 2021;599:120417.
22. Lafeber I, Tichem JM, Ouwerkerk N, van Unen AD, van Uitert JJD. Bijleveld-Olierook H.C.M., et al. 3D printed furosemide and sildenafil tablets: innovative production and quality control. *Int J Pharm*. 2021;603:120694.
23. Bendicho-Lavilla C, Rodríguez-Pombo L, Januskaite P, Rial C, Alvarez-Lorenzo C. Basit A.W., et al. Ensuring the quality of 3D printed medicines: integrating a balance into a pharmaceutical printer for in-line uniformity of mass testing. *J Drug Deliv Sci Technol*. 2024;92:105337.
24. dos Santos J, Balbinot GdS, Buchner S, Collares FM, Windbergs M, Deon M, et al. 3D printed matrix solid forms: can the drug solubility and dose customisation affect their controlled release behaviour? *Int J Pharm X*. 2023;5:100153.
25. Markl D, Zeitler JA, Rasch C, Michaelsen MH, Müllertz A, Rantanen J, et al. Analysis of 3D prints by X-ray computed microtomography and terahertz pulsed imaging. *Pharm Res*. 2017;34(5):1037–1052.
26. Reich G. Near-infrared spectroscopy and imaging: basic principles and pharmaceutical applications. *Adv Drug Deliv Rev*. 2005;57(8):1109–1143.
27. Paudel A, Raijada D, Rantanen J. Raman spectroscopy in pharmaceutical product design. *Adv Drug Deliv Rev*. 2015;89:3–20.
28. Beć KB, Grabska J, Siesler HW, Huck CW. Handheld near-infrared spectrometers: where are we heading? *NIR News*. 2020;31(3–4):28–35.
29. Crocombe RA. Portable spectroscopy. *Appl Spectrosc*. 2018;72(12):1701–1751.
30. Casian T, Gavan A, Iurian S, Porfire A, Toma V, Stiufiuc R, et al. Testing the limits of a portable NIR spectrometer: content uniformity of complex powder mixtures followed by calibration transfer for in-line blend monitoring. *Molecules*. 2021;26(4):1129.
31. Beć KB, Grabska J, Huck CW. Principles and applications of miniaturized near-infrared (NIR) spectrometers. *Chem A Eur J*. 2021;27(5):1514–1532.
32. Seoane-Viaño I, Xu X, Ong JJ, Teyeb A, Gaisford S, Campos-Álvarez A, et al. A case study on decentralized manufacturing of 3D printed medicines. *Int J Pharm X*. 2023;5:100184.
33. Pollard TD, Seoane-Viaño I, Ong JJ, Januskaite P, Awwad S, Orlu M, et al. Inkjet drug printing onto contact lenses: deposition optimisation and non-destructive dose verification. *Int J Pharm X*. 2023;5:100150.
34. Yang TL, Stogiannari M, Janeczko S, Khoshan M, Lin Y, Isreb A, et al. Towards point-of-care manufacturing and analysis of immediate-release 3D printed hydrocortisone tablets for the treatment of congenital adrenal hyperplasia. *Int J Pharm*. 2023;642:123072.
35. Yang TL, Szewc J, Zhong L, Leonova A, Giebultowicz J, Habashy R, et al. The use of near-infrared as process analytical technology (PAT) during 3D printing tablets at the point-of-care. *Int J Pharm*. 2023;642:123073.
36. Ahola I, Tomberg T, Cornett C, Strachan C, Rantanen J, Genina N. Understanding the complexity of near-infrared quantification of highly porous patient-tailored drug

products by utilizing chemometrics and stimulated Raman imaging. *Int J Pharm*. 2025;671:125205.
37. Denis L, Jørgensen AK, Do B, Vaz-Luis I, Pistilli B, Rieutord A, et al. Developing an innovative 3D printing platform for production of personalised medicines in a hospital for the OPERA clinical trial. *Int J Pharm*. 2024;661(124306).
38. Lorizio W, Wu AH, Beattie MS, Rugo H, Tchu S, Kerlikowske K, et al. Clinical and biomarker predictors of side effects from tamoxifen. *Breast Cancer Res Treat*. 2012;132(3):1107–1118.
39. Mao D, Hachem H, Chang H, Dima D, Dower J, Wismer M, et al. Treatment interruption and discontinuation of hormonal therapy in hormone receptor-positive breast cancer patients. *Breast Cancer Res Treat*. 2020;184(3):665–674.
40. Wilkinson L, Gathani T. Understanding breast cancer as a global health concern. *Br J Radiol*. 2022;95(1130), 20211033.
41. He W, Eriksson M, Eliasson E, Grassmann F, Bäcklund M, Gabrielson M, et al. CYP2D6 genotype predicts tamoxifen discontinuation and drug response: a secondary analysis of the KARISMA trial. *Ann Oncol*. 2021;32(10):1286–1293.
42. Zembutsu H. Pharmacogenomics toward personalized tamoxifen therapy for breast cancer. *Pharmacogenomics*. 2015;16(3):287–296.
43. Kiyotani K, Mushiroda T, Imamura CK, Tanigawara Y, Hosono N, Kubo M, et al. Dose-adjustment study of tamoxifen based on CYP2D6 genotypes in Japanese breast cancer patients. *Breast Cancer Res Treat*. 2012;131(1):137–145.
44. Khalaj Z, Baratieh Z, Nikpour P, Schwab M, Schaeffeler E, Mokarian F, et al. Clinical trial: CYP2D6 related dose escalation of tamoxifen in breast cancer patients with Iranian ethnic background resulted in increased concentrations of Tamoxifen and its metabolites. *Front Pharmacol*. 2019:10:530.
45. Goldberg I, Becker Y. Polymorphs of tamoxifen citrate: detailed structural characterization of the stable form. *J Pharm Sci*. 1987;76(3):259–264.
46. Fawcett TG, Gates-Rector S, Gindhart AM, Rost M, Kabekkodu SN, Blanton JR, et al. A practical guide to pharmaceutical analyses using X-ray powder diffraction. *Powder Diffr*. 2019;34(2):164–183.
47. Gamberini MC, Baraldi C, Tinti A, Palazzoli F, Ferioli V. Vibrational study of tamoxifen citrate polymorphism. *J Mol Struct*. 2007;840(1):29–37.
48. Awotunde O, Lu J, Cai J, Roseboom N, Honegger S, Joseph O, et al. Mitigating the impact of gelatin capsule variability on detection of substandard and falsified pharmaceuticals with near-IR spectroscopy. *Anal Methods*. 2024;16(11):1611–1622.
49. Si L, Ni H, Pan D, Zhang X, Xu F, Wu Y, et al. Nondestructive qualitative and quantitative analysis of Yaobitong capsule using near-infrared spectroscopy in tandem with chemometrics. *Spectrochim Acta Part A Mol Biomol Spectrosc*. 2021;252:119517.
50. Mainka DL, Link A. Near-infrared spectroscopic identification and quantification of active pharmaceutical ingredients in closed capsules: a feasibility study for pediatric doses. *Anal Methods*. 2019;11(40):5185–5194.
51. Eilers PH, Boelens HF. Baseline correction with asymmetric least squares smoothing. *Leiden Univ Med Cent Rep*. 2005;1(1):5.
52. Hargreaves MD, Macleod NA, Smith MR, Andrews D, Hammond SV, Matousek P. Characterisation of transmission Raman spectroscopy for rapid quantitative analysis of intact multi-component pharmaceutical capsules. *J Pharm Biomed Anal*. 2011;54(3):463–468.
53. Cordero E, Latka I, Matthäus C, Schie I, Popp J. In-vivo Raman spectroscopy: from basics to applications. *J Biomed Opt*. 2018;23(7):1–23.
54. Alula MT, Mengesha ZT, Mwenesongole E. Advances in surface-enhanced Raman spectroscopy for analysis of pharmaceuticals: a review. *Vib Spectrosc*. 2018;98:50–63.
55. Metrohm. MIRA M-1 advanced package [Internet]. Available from: https://www.metrohm.com/en_gb/products/2/9230/29230020.html. [Accessed 01 July 2025].
56. Eliasson C, Macleod NA, Jayes LC, Clarke FC, Hammond SV, Smith MR, et al. Non-invasive quantitative assessment of the content of pharmaceutical capsules using transmission Raman spectroscopy. *J Pharm Biomed Anal*. 2008;47(2):221–229.
57. Johansson J, Sparén A, Svensson O, Folestad S, Claybourn M. Quantitative transmission Raman spectroscopy of pharmaceutical tablets and capsules. *Appl Spectrosc*. 2007;61(11):1211–1218.
58. Matousek P, Parker AW. Non-invasive probing of pharmaceutical capsules using transmission Raman spectroscopy. *J Raman Spectrosc*. 2007;38(5):563–567.
59. Kauffman JF, Dellibovi M, Cunningham CR. Raman spectroscopy of coated pharmaceutical tablets and physical models for multivariate calibration to tablet coating thickness. *J Pharm Biomed Anal*. 2007;43(1):39–48.
60. Remoto PJG, Gordon KC, Fraser-Miller SJ. A quantitative chemometric study of pharmaceutical tablet formulations using multi-spectroscopic fibre optic probes. *Pharmaceuticals*. 2024;17(12):1659.
61. Barnes RJ, Dhanoa MS, Lister SJ. Standard normal variate transformation and de-trending of near-infrared diffuse reflectance spectra. *Appl Spectrosc*. 1989;43(5):772–777.
62. Roger JM, Mallet A, Marini F. Preprocessing NIR spectra for aquaphotomics. *Molecules*. 2022;27(20):6795.
63. Rinnan Å, van den Berg F, Engelsen SB. Review of the most common pre-processing techniques for near-infrared spectra. *TrAC Trends Anal Chem*. 2009;28(10):1201–1222.
64. Geravand A, Hashemi Nezhad SM. Simulation study of the orbital raster scan (ORS) on the raman spectroscopy. *Optik*. 2019;178:83–89 (Stuttg).
65. Jones RR, Hooper DC, Zhang L, Wolverson D, Valev VK. Raman techniques: fundamentals and frontiers. *Nanoscale Res Lett*. 2019;14(1):231.
66. Rady A, Fischer J, Reeves S, Logan B, James Watson N. The effect of light intensity, sensor height, and spectral pre-processing methods when using NIR spectroscopy to identify different allergen-containing powdered foods. *Sensors*. 2020;20(1).
67. Yang W, Knorr F, Popp J, Schie IW. Development and evaluation of a hand-held fiber-optic Raman probe with an integrated autofocus unit. *Opt Express*. 2020;28(21):30760–30770.
68. U.S. Food and DrugAdministration. Distributed Manufacturing and Point-of-Care Manufacturing of Drugs - Discussion Paper. Maryland: Silver Spring; 2022:20993. US.
69. U.K. Medicines and Healthcare products Regulatory Agency. Consultation on point of care manufacturing. 2021.
70. U.K. Medicines and Healthcare products Regulatory Agency. Consultation on point of care manufacturing: consultation outcome. 2023.
71. European Medicines Agency. Quality Innovation Group, (2022).
72. U.K. Statutory Instruments. The Human Medicines (Amendment) (Modular Manufacture and Point of Care) Regulations 2025, (2025).
73. Mora-Castaño G, Rodríguez-Pombo L, Carou-Senra P, Januskaite P, Rial C, Bendicho-Lavilla C, et al. Optimising 3D printed medications for rare diseases: in-line mass uniformity testing in direct powder extrusion 3D printing. *Int J Pharm*. 2025;668:124964.
74. Krueger L, Awad A, Basit AW, Goyanes A, Miles JA, Popat A. Clinical translation of 3D printed pharmaceuticals. *Nat Rev Bioeng*. 2024;2:801-803.
75. Ntziouni A, Thomson J, Xiarchos I, Li X, Bañares MA, Charitidis C, et al. Review of existing standards, guides, and practices for Raman spectroscopy. *Appl Spectrosc*. 2022;76(7):747–772.